

Conductance of bilayer graphene in the presence of a magnetic field: Effects of disorder

H. Hatami,¹ N. Abedpour,² A. Qaiumzadeh,^{2,3} and Reza Asgari^{2,*}

¹*Department of Physics, University of Tabriz, Tabriz 51665-163, Iran*

²*School of Physics, Institute for Research in Fundamental Sciences, (IPM) Tehran 19395-5531, Iran*

³*Institute for Advanced Studies in Basic Sciences (IASBS), Zanjan 45195-1159, Iran*

We investigate the electronic transport properties of unbiased and biased bilayer graphene nanoribbon in n-p and n-n junctions subject to a perpendicular magnetic field. Using the non-equilibrium Green's function method and the Landauer-Büttiker formalism, the conductance is studied for the cases of clean, on-site, and edge disordered bilayer graphene. We show that the lowest Hall plateau remains unchanged in the presence of disorder, whereas asymmetry destroys both the plateaus and conductance quantization. In addition, we show that disorder induces an enhancement of the conductance in the n-p region in the presence of magnetic fields. Finally, we show that the equilibration of quantum Hall edge states between distinctively doped regions causes Hall plateaus to appear in the regime of complete mode mixing.

PACS numbers: 73.63.-b, 72.80.Ng, 81.05.ue, 05.60.Gg

I. INTRODUCTION

In recent years, after the success of fabrication of both monolayer¹ and multilayer graphene sheets²⁻⁴, there has been a lot of interest in the transport properties of graphene nano-ribbons, especially the behavior of low-energy charge carrier excitations⁵⁻⁷. Ideal monolayer graphene is a gapless semimetal with zero density of states at the Dirac points. The low-energy electronic excitations in the vicinity of the Dirac points have linear dispersions, and are described by an effective massless Dirac Hamiltonian. The low-energy electrons in bilayer graphene, on the other hand, have a quadratic dispersion relation. Both for monolayer and bilayer graphene, the wave functions are composed of two sublattices A and B , and give rise to the chirality of the charge carriers. Therefore, the charge carriers in graphene are chiral and has awoken an enormous interest in graphene, for instance with regards of effects such as the Berry phase, which is π in monolayer graphene and 2π in bilayer graphene. Although intrinsic bilayer graphene is a zero-gap semimetal, it exhibits very interesting properties when a gate voltage is applied, which makes bilayer graphene into a tunable band gap semiconductor^{8,9}. The band gap determines the threshold voltage and the on-off ratio of field effect transistors and diodes. Therefore, bilayer graphene is more convenient for applications in nano-electronic industry than monolayer graphene¹⁰.

One of the exotic phenomena that has been observed in monolayer and bilayer graphene is the anomalous quantum Hall effect^{1,11}. The nature of massless chiral Dirac charge carriers in monolayer graphene gives rise to this property of the Hall plateaus, that behave as $\sigma_{xy} = \pm\sigma_0(N + 1/2)$, with N being the Landau level index and $\sigma_0 = 4e^2/h$. The factor of 4 originates from the valley and spin degeneracies. In undoped bilayer graphene, the sequence of Hall plateaus, with $\sigma_{xy} = \pm\sigma_0 N$, were observed. The first plateau at $N = 0$ is missing which implies that bilayer graphene is metallic at the neutrality point, while the standard quantum Hall effect in bilayer graphene can be recovered by applying a gate voltage. The quantum Hall states, fully quantized due to the presence of a magnetic field, as well as broken-symmetry states at intermediate filling factors such 0, ± 1 , ± 2 and ± 3 , were experimentally observed by Feldman *et al.*¹².

In a perfect nanoribbon, the electron transmission via subbands due to lateral confinement of the electronic states implies the quantization of the conductance in units of $G_0 = 2e^2/h$.¹³ Recently, the zero-temperature conductance of free-disordered monolayer and unbiased bilayer graphene nanoribbons in the presence of a uniform perpendicular magnetic field was calculated¹⁴. The conductance in monolayer graphene nanoribbon is given by $2(n + 1/2)G_0$ for the case of zigzag edges, and nG_0 for the case of armchair edges. On the other hand, it was shown that in a bilayer graphene nanoribbon the conductance is quantized as $2(n + 1)G_0$ for zigzag edges, and nG_0 for armchair edges, where n is an integer.

The quantum Hall effect and quantized transport in graphene junctions in the bipolar (p-n), and unipolar (n-n or p-p) regimes was investigated theoretically and experimentally by several groups^{15,16}. Long, *et al.*¹⁵ by using the Landauer-Buttiker formalism, showed that on-site disorder induces the enhancement of the transport in monolayer graphene p-n junctions in the presence of a magnetic field. On the other hand, they showed that in the n-n junction, the lowest plateau survives in a sufficiently broad range of on-site disorder strengths. They also showed that in a particular range of disorder strengths new plateaus (*i.e.* $G = 3e^2/h$ and e^2/h) emerge^{15,17}, something also observed experimentally.

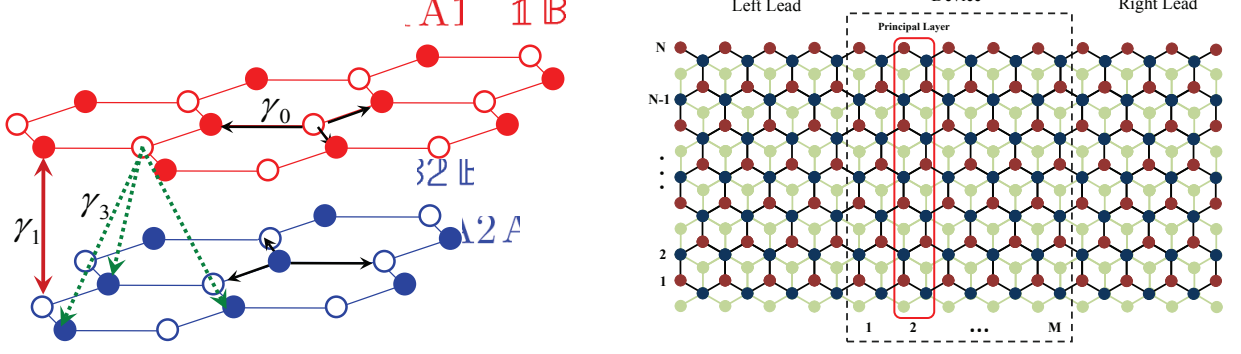


FIG. 1: (Color online)(Left): Schematic 3D view of bilayer graphene incorporating all coupling energies. (Right): Schematic picture of zBG NR with length M and width N atoms, and the definition of the principal layer.

Transport measurements in high quality bilayer graphene pnp junctions have also been performed, and electron mobilities up to $10000 \text{ cm}^2/(\text{V s})$ have been measured for gapless systems, and an on-off ratio up to 20000 for gapped systems.¹⁸ Moreover, the fractional-valued quantum Hall plateaus due to equilibration of quantum Hall edge states between distinctively doping regions have been observed.¹⁸ Consequently, the conductance exhibits plateaus arising from the mixing of edge states at the interfaces.

In this paper, we investigate the conductance of the chiral massive carrier in the presence of a uniform perpendicular magnetic field, both for unbiased and biased bilayer graphene nanoribbons configured as n-n and n-p junctions^{18,19}. In addition, we study the influence of on-site and edge disorders on the conductance. For these purposes, we use the tight-binding model and Landauer-Büttiker formalism together with the non-equilibrium Green's function approach²⁰. It should be noted that, in general, the absolute magnitude of the magnetic field can cause reflection at the boundaries of the electronic devices²¹. We restrict our attention in this article to the case of a system in which the reflection on the boundaries due to the magnetic field can be ignored.

The paper is organized as follows. In Sec. II, we introduce our model and formalism, such as the tight-binding Hamiltonian for bilayer graphene junction, and a recursive method for calculating the Green's function. In Sec. III, our numerical results for the conductance of disordered and biased bilayer graphene junctions in the presence of magnetic field are presented. Finally, we conclude in Sec. IV with a brief summary.

II. MODEL AND METHOD

We consider a bilayer graphene ribbon with Bernal stacking (AB)²², as a conductor connected to the left and the right leads as depicted in Fig. 1. The model Hamiltonian is given by,

$$H = H_{center} + H_L + H_R \quad (1)$$

where H_{center} , H_L and H_R are the Hamiltonian of the center region, the left and the right leads, respectively. Two leads are considered as perfect semi-infinite bilayer graphene nanoribbons. Notice that the leads are also structured by the Bernal stacking bilayer graphene. We consider the nearest-neighbor tight-binding Hamiltonian with one π -orbital per site on the lattice. The effective one-body Hamiltonian of bilayer graphene in the presence of the magnetic field is given as follows,

$$\begin{aligned} H = & -\gamma_0 \sum_{l, \langle i, j \rangle} (e^{i\phi_{i,j}} a_{l,i}^\dagger b_{l,j} + h.c.) \\ & - \gamma_1 \sum_i (a_{1,i}^\dagger b_{2,i} + h.c.) - \gamma_3 \sum_{\langle i, j \rangle} (e^{i\phi_{i,j}} b_{1,i}^\dagger a_{2,j} + h.c.) \\ & + \sum_{l,i} v_l (a_{l,i}^\dagger a_{l,i} + b_{l,i}^\dagger b_{l,i}) \\ & + \sum_{l,i} [(w_i + (-1)^l \Delta) (a_{l,i}^\dagger a_{l,i} + b_{l,i}^\dagger b_{l,i})] \end{aligned} \quad (2)$$

where $a_{l,i}^\dagger$ and $a_{l,i}$ ($b_{l,i}^\dagger$ and $b_{l,i}$) are the creation and annihilation operators at sublattice A (B) in the layer $l = 1, 2$ at the i th site, respectively. The intralayer nearest-neighbor hopping energy is $\gamma_0 = 3.16\text{eV}$, the hopping energy between on-top sublattices A and B in different layers is $\gamma_1 = 0.39\text{eV}$ and furthermore, $\gamma_3 = 0.315\text{eV}$ denotes the hopping energy between not on-top sublattices A and B between two layers⁸. Another hopping energy between the nearest-neighboring layers, $\gamma_4 = 0.04\text{eV}$, is very small compare to γ_0 and can be ignored. In the presence of the external perpendicular magnetic field \mathbf{B} , the hopping integral acquires the Peierls phase factor given by $e^{i\phi_{i,j}}$ where $\phi_{i,j} = \int_i^j \mathbf{A} \cdot d\mathbf{l} / \phi_0$, with the magnetic flux quantum $\phi_0 = \hbar/e$. We use the Landau gauge as $\mathbf{A} = (-By, 0, 0)$. The applied magnetic field is considered to be only on the center region. $v_{l,i}$ reduces to the bias voltage E_L (E_R) on the left (right) lead and can be controlled by the gate voltage. The electrostatic potential changes from the right lead to the left lead and is assumed to be linear as $v_l = k(E_R - E_L)/(M + 1) + E_L$, $k = 1, 2, \dots, M$, where M is the length of the center region (see Fig. 1). We consider on-site disorder w_i , being a random variable with a uniform distribution in an interval $[-W/2, W/2]$ with the disorder strength W which exists only in the center region. The size of the central region, *i.e.* conductor, is given by $4N \times M$ atoms. Here we define the asymmetric between two layers, Δ , indicating the difference between on-site energies. The current can be calculated from the Landauer-Büttiker formula²⁰ as

$$I = \frac{2e}{h} \int d\epsilon T_{LR}(\epsilon) [f_L(\epsilon) - f_R(\epsilon)] \quad (3)$$

where $f_\alpha(\epsilon) = 1/(\exp[(\epsilon - eV_\alpha)/k_B T] + 1)$, ($\alpha = L, R$), is the Fermi distribution function in the leads. To calculate the transmission coefficient $T_{LR}(\epsilon)$, we use

$$T_{LR}(\epsilon) = \text{Tr}[\Gamma_L G \Gamma_R G^\dagger] \quad (4)$$

where the line width function Γ_α , that describes the coupling between the conductor and the leads is given by

$$\Gamma_\alpha(\epsilon) = i[\Sigma_\alpha^r(\epsilon) - \Sigma_\alpha^a(\epsilon)], \quad (5)$$

in which the retarded Green's functions is written as

$$G(\epsilon) = \frac{1}{\epsilon - H_{\text{center}} - \Sigma_L^r(\epsilon) - \Sigma_R^a(\epsilon)} \quad (6)$$

The retarded self-energy Σ_α^r , due to the coupling to α -th lead is

$$\begin{aligned} \Sigma_L^r &= h_{LC}^\dagger (\epsilon - H_L)^{-1} h_{LC} \\ \Sigma_R^r &= h_{CR} (\epsilon - H_R)^{-1} h_{CR}^\dagger \end{aligned} \quad (7)$$

where h_{LC} (h_{CR}) is the hopping Hamiltonian from the left lead to the center region (from center region to the right lead) and $G_\alpha = (\epsilon - H_\alpha)^{-1}$ can be calculated by an iterative method numerically^{23,24}. We assume an infinite stack of principal layers with the nearest-neighbor interactions. A principle layer is defined as the smallest group of neighbouring atoms planes such way that only nearest-neighbour interactions exist between principle layers (see Fig. 1). Thus, we can transform the original system into a linear chain of the principal layers. By using this approach, we write the matrix elements of $(\epsilon - H)G = 1$ in the following form²⁵

$$\begin{aligned} (\epsilon - H_{00})G_{0,0} &= 1 + H_{01}G_{1,0} \\ (\epsilon - H_{00})G_{1,0} &= H_{01}^\dagger G_{0,0} + H_{01}G_{2,0} \\ &\dots \\ (\epsilon - H_{00})G_{n,0} &= H_{01}^\dagger G_{n-1,0} + H_{01}G_{n+1,0} \end{aligned} \quad (8)$$

in which H_{00} and H_{01} describe the coupling within the principal layer and the adjacent principal layers, respectively. For simplicity, we assume that $H_{00} = H_{11} = H_{22} \dots$ and $H_{01} = H_{12} = H_{23} \dots$. Notice that G_{nm} is the matrix element of the Green's function between the principal layers. It is easy to obtain an iterative set of equations for $G_{n,0}$

$$G_{n,0} = t_i G_{n-2^i,0} + \tilde{t}_i G_{n+2^i,0} \quad (9)$$

for $n \geq 2^i$, where

$$\begin{aligned} t_i &= (1 - t_{i-1}\tilde{t}_{i-1} - \tilde{t}_{i-1}t_{i-1})^{-1}t_{i-1}^2 \\ \tilde{t}_i &= (1 - t_{i-1}\tilde{t}_{i-1} - \tilde{t}_{i-1}t_{i-1})^{-1}\tilde{t}_{i-1}^2 \end{aligned} \quad (10)$$

where

$$\begin{aligned} t_0 &= (\epsilon - H_{00})^{-1} H_{01}^\dagger \\ \tilde{t}_0 &= (\epsilon - H_{00})^{-1} H_{01} \end{aligned} \quad (11)$$

then we can write

$$\begin{aligned} G_{1,0} &= t_0 G_{0,0} + \tilde{t}_0 G_{2,0} \\ &= (t_0 + \tilde{t}_0 t_1) G_{0,0} + \tilde{t}_1 G_{4,0} \\ &\dots \\ &= (t_0 + \tilde{t}_0 t_1 + \dots + \tilde{t}_0 \dots \tilde{t}_{n-1} t_n) G_{0,0} + \tilde{t}_n G_{2n+1,0} \end{aligned} \quad (12)$$

We solve Eq. (9) iteratively. This process is repeated until $t_{n+1}, \tilde{t}_{n+1} < \varepsilon$, in which ε is a tiny value and is chosen as small as one pleases. Therefore $G_{2n+1,0} \simeq 0$, and the transfer matrix is thus given by $T = t_0 + \tilde{t}_0 t_1 + \tilde{t}_0 \tilde{t}_1 t_2 + \dots + \tilde{t}_0 \dots \tilde{t}_{n-1} t_n$. Accordingly, we can write $G_{1,0} = T G_{0,0}$ and $G_{0,0} = \tilde{T} G_{1,0}$. The self-energies of the conductor-leads are $\Sigma_L = H_{01}^\dagger \tilde{T}$ and $\Sigma_R = H_{01} T$. Finally, the zero-temperature conductance $G = \lim_{V \rightarrow 0} \frac{dI}{dV}$, can be obtained by using the Landauer-Büttiker formalism as²⁰

$$G = \frac{2e^2}{h} T_{LR}(\epsilon_F). \quad (13)$$

III. NUMERICAL RESULTS

In this Section, we present our numerical results for zero-temperature conductance of unbiased and biased zBGNR in the presence of a magnetic field as well as various types of disorders. We assume that the width of the nanoribbons is $N = 45$, the voltage of the left lead is $E_L = -0.2$. All the energies are in units of γ_0 . We neglect the effect of the Zeeman splitting and the spin-orbit interaction, which are important only at very low energies, at which disorder effects normally dominate.⁵ We define dimensionless magnetic field as $\phi \equiv (3\sqrt{3}/4)a^2 B/\phi_0$, where 2ϕ is the magnetic flux in a honeycomb lattice.

In connection with the formation of the Hall plateaus, it is necessary to consider ribbons with width greater than the magnetic length scale, $l_B = \sqrt{\hbar/eB}$. We consider $\phi = 0.01$ corresponds to $l_B \approx 15\text{\AA}$ which is smaller than the considered ribbon size with width $L_y(N = 45) \approx 10\text{nm}$, and length $L_x(M = 21) \approx 5.5\text{nm}$.

The conductance of unbiased clean zBGNR as a function of E_R is shown in Fig. 2 for various sizes, both in the absence ($\phi = 0$) and presence ($\phi = 0.01$) of a magnetic field. In the absence of a magnetic field, the conductance in the n-n region ($E_R < 0$) is quantized due to transverse confinement of the ribbon, and well described by $G = 2(n+1)G_0$, with the minimum conductance of a zBGNR being $2G_0$ ¹⁴. Moreover, the conductance is independent of the ribbon length at low E_R values. As one can see in the n-n region for $\phi = 0$, the energy spacings between plateaus are not equidistant (whereas in monolayer graphene they are), because of the quadratic dispersion relation. The widths of the conductance steps are related to the energy scale between the successive modes in the energy spectrum. Therefore the conductance is sensitive to E_L values, and the number of plateaus increases with increasing bias voltage, *i.e.* $|E_L - E_R|$. Also for $E_R < E_L$ there are no plateaus, identical to the case of monolayer graphene¹⁵. In the n-p region, $E_R > 0$, the conductance occurs due to the chiral charge carriers tunneling between n and p regions, and the conductance is always less than the corresponding plateau value in the n-n region. In this region the conductance decreases with increasing length of the ribbon M , since the number of scattering centers increases.

The effect of a high magnetic field, $\phi = 0.01$ on the conductance of a clean graphene junction in unipolar and bipolar regimes is shown in Fig. 2. In the n-p region the length dependence of the Peierls phase factor gives rise to a non-monotonic behavior of the conductance as a function of the length and energy E_R , noticeably at very low E_R values. This behavior is in contrast with the result obtained for the zero magnetic field. Our results show that the conductance of the clean sample in bipolar regime is suppressed dramatically in the presence of the magnetic field. However, the first and the second Hall plateaus survive (*i.e.* $G/G_0 = 2$ and 4) in the n-n region.

We also study the effect of asymmetry between two layers, Δ , *i.e.* when the two layers have different on-site energies. The asymmetry here leads to the opening of a gap between the conduction and valance bands. In Fig. 3, we plot the conductance of a free-disordered zBGNR as a function of E_R in the absence of the magnetic field. In the n-n region, asymmetry leads to a decrease of the conductance, while in the n-p region, asymmetry results in an enhancement of the conductance. This effect can be described based on the channels of the charge carriers. In the n-n region, electrons are only charge carriers while in the n-p region, because of the existence of asymmetry between two layers, one layer is n-doped and the other is p-doped. Accordingly, both electrons and holes play a role in the transport. In the n-n

region, the conductance fluctuations occur for low $|E_R|$ and increase with length size M . Importantly, opening a gap affects the transversal confinement and the quantized steps are destroyed by asymmetry in the n-n region.

The conductance of a zBGNR for various Δ is plotted in Fig. 4. The asymmetry leads to an increase of the conductance in the n-p region, and a decrease in the n-n region. The conductance fluctuations increase with increasing Δ values. In the right panel of Fig. 4 we show the effect of the magnetic field on the conductance in the presence of asymmetry. In the n-n region the Hall plateaus are destroyed by asymmetry and accordingly the conductance reduces. On the other hand, in the n-p region asymmetry leads to increasing conductance.

We are now in the position to introduce some disorder and study the effects of disorder on the conductance of zBGNR in the presence of a magnetic field B . We consider the effect of on-site disorder on the conductance with a uniform disorder distribution in the range of $[-W/2, W/2]$. In Fig. 5, we plot the conductance as a function of E_R for the various W for $\phi = 0$ (left panel). The number of realizations is 200. In the n-n region, the conductance is suppressed. In the n-p region at low E_R values, the conductance increases when the strength of disorder increases. The conductance is independent of disorder in the large positive E_R regions.

We also consider a disordered zBGNR in the presence of the high perpendicular magnetic field. The quantum Hall effect in gapless bilayer graphene occurs at the filling factors $\nu = \pm 1, \pm 2, \pm 3, \dots$, in which there are $|\nu| = |n_0 h/eB|$ edge modes propagating in the opposite directions at $\nu > 0$ and $\nu < 0$. Here n_0 is the charge density. The conductance plateaus for unipolar regime is given by $G_{nn}/G_0 = G_{pp}/G_0 = 2(\min(|\nu_L|, |\nu_R|)) = 2, 4, 6, \dots$ and for a bipolar system the conductance is $G_{pn}/G_0 = 2(\frac{|\nu_L||\nu_R|}{|\nu_L|+|\nu_R|}) = 1, \frac{4}{3}, \frac{3}{2}, 2, \dots$ in the two-terminal ohmic regime.^{16,18} It is worthwhile mentioning that those expressions can also be applied to monolayer nanoribbons in the ohmic regime since these two materials have similar resistivities and thus also similar mean free paths²⁶.

For the unipolar regime the edge states which are common between the left and right regions propagate between the two leads, while $|\nu_L - \nu_R|$ states do not contribute to the conductance. In the bipolar regime, on the other hand, mode mixing occurs in the interface of two regions and for complete mode mixing the conductance plateaus obey the aforementioned formula for G_{pn}/G_0 . In unipolar regime our numerical calculations show that ($\phi = 0.01$, right panel) the lowest Hall plateaus remain unchanged in the presence of small disorder strengths, whereas the Hall plateaus are destroyed with increasing disorder strengths. We see perfect Hall plateaus in the unipolar regime with no equidistance in the scale of E_R . In the clean bipolar regime the Hall edge states are separated for electrons and holes, and leads to suppression of the conductance. In addition, small strengths of on-site disorder induce the enhancement of the conductance of zBGNR in the presence of a magnetic field in the n-p region. At small strengths of disorder, $W < 1$, in the n-p region, the conductance is enhanced due to the mixture of electron and hole edge states. Thus in the bipolar regime, mode mixing at interface leads to two-terminal conductances. On the other hand, for large values of disorder strength, the system enters the insulating regime and the conductance is very small for all E_L and E_R . We expect that the lowest Hall plateau survives only within certain range of disorder strengths. In the inset of Fig. 5 the conductance is shown in the ohmic regime and it obeys $G_{pn}/G_0 = 2(\frac{|\nu_L||\nu_R|}{|\nu_L|+|\nu_R|}) = 1, \frac{4}{3}, \frac{3}{2}, 2, \dots$, the edge state equilibration condition. It should be noted that the ohmic behavior has been observed experimentally in bilayer graphene pnp junctions as well as graphene p-n junctions^{16,18}. Our numerical results are in excellent agreement with the recent experiment.

We also investigate the effect of asymmetry in the presence of on-site disorder and our results are shown in Fig. 6. The Hall plateaus are destroyed by asymmetry even for very low disorder strengths. Also, asymmetry destroys finite size quantization of the conductance in the n-n region. The strong fluctuations vanish in the n-n region for small E_R values and in the presence of disorder, as is shown in Fig. 6 for the case of $\phi = 0$.

Another type of disorder which is indispensable in real nanoribbons is edge disorder²⁷. This type of disorder is generated by eliminating carbon atoms randomly along the edges of GNR. Note that because of our limitations in this approach, we consider only one layer depth edge disorder. In Fig. 7, we have shown the effect of edge disorder on the conductance of zBGNR as a function of E_R for two different nanoribbon lengths M . The conductance increases in the n-p region at low E_R as compared to the clean system, and it is independent of disorder in large E_R . It is important to investigate the persistence of the Hall conductance plateaus versus edge disorder. As we have shown in Fig. 7, the Hall plateaus remain unchanged in the presence of edge disorder as well as on-site disorder for $\phi = 0.01$.

IV. SUMMARY AND CONCLUSION REMARKS

In summary, we studied the effect of on-site and edge disorder on the conductance of biased zigzag bilayer graphene nanoribbon subject to a uniform perpendicular magnetic field. Our approach was based on the non-equilibrium Green's function method and Landauer-Büttiker formalism. Our results show that the lowest Hall plateaus can survive in the presence of a broad range of disorder strengths in the n-n region, while an asymmetry between two layers destroys them. On the other hand, disorder induces an enhancement of the conductance in the presence of the

magnetic field in the n-p region. In addition, the conductance is enhanced due to asymmetry in the n-p region. We also showed that the Hall plateaus appear due to equilibration of the quantum Hall edge states in the different regions with electron and hole type charge carriers.

Our approach can be extended to long-range disorder due to charge impurities, and also to the case of spin dependence of the electronic transport with ferromagnetic-gate in bilayer graphene nanoribbon sheets.

V. ACKNOWLEDGEMENT

We acknowledge useful discussions with A. G. Moghaddam and H. Hassanian. We would also like to acknowledge M. Jääskeläinen for carefully reading our manuscript. A. Q. has been supported partially by IPM grant.

-
- * Electronic address: asgari@ipm.ir
- ¹ K. S. Novoselov, A. K. Geim, S. V. Morozov, D. Jiang, Y Zhang, S. V. Dubonos, I. V. Grigorieva, and A. A. Firsov, *Science* **306**, 666 (2004) .
 - ² C. Berger, Z. Song, T. Li, X. Li, A. Y. Ogbazghi, R. Feng, Z. Dai, A. N. Marchenkov, E. H. Corad and P. N. First, *J. Phys. Chem. B* **108**, 19912 (2004) .
 - ³ K. S. Novoselov, A. K. Geim, S. V. Morozov, D. Jiang, M. I. Katsnelson, I. V. Grigorieva, S. V. Duboson and A. A. Firsov, *Nature (London)* **438**, 197 (2005) .
 - ⁴ Y. Zhang, Y.-W. Tan, H. L. Stormer and P. Kim, *Nature (London)* **438**, 201 (2005) .
 - ⁵ A. H. Castro Neto, F. Guinea, N. M. Peres, K. S. Novoselov, and A. K. Geim, *Rev. Mod. Phys.* **81**, 109 (2009) .
 - ⁶ Eduardo V. Castro, K. S. Novoselov, S. V. Morozov, N. M. R. Peres, J. M. B. Lopes dos Santos, Johan Nilsson, F. Guinea, A. K. Geim, A. H. Castro Neto, *J. Phys.: Condens. Matter*, **22**, 175503 (2010) .
 - ⁷ Johan Nilsson, A. H. Castro Neto, F. Guinea, N. M. R. Peres, *Phys. Rev. B* **78**, 045405 (2008) .
 - ⁸ A. B. Kuzmenko, et al. *Phys. Rev. B* **80**, 165406 (2009) .
 - ⁹ Kin Fai Mak, Chun Hung Lui, Jie Shan, Tony F. Heinz, *Phys. Rev. Lett.* **102**, 256405(2009) .
 - ¹⁰ Taisuke Ohta, Aaron Bostwick, Thomas Seyller, Karsten Horn, Eli Rotenberg, *Science* **313**, 951 (2006); Eduardo V. Castro, K. S. Novoselov, S. V. Morozov, N. M. R. Peres, J. M. B. Lopes dos Santos, Johan Nilsson, F. Guinea, A. K. Geim, A. H. Castro Neto, *Phys. Rev. Lett.* **99**, 216802 (2007); J.B. Oostinga, H.B. Heersche, X. Liu, A.F. Morpurgo, L.M.K. Vandersypen, *Nature Mater.* **7**, 151 (2008); W. Yao, D. Xiao, and Q. Niu, *Phys. Rev. B* **77**, 235406 (2008) .
 - ¹¹ K. S. Novoselov, E. McCann, S. V. Morozov, V. I. Falko, M. I. Katsnelson, U. Zeitler, D. Jiang, F. Schedin and A. K. Geim, *Nature physics* **2**, 177 (2006); E. McCann and V. I. Falko, *Phys. Rev. Lett.* **96**, 086805 (2006); Ya-Fen Hsu, Guang-Yu Guo, *Phys. Rev. Lett.* **82**, 165404 (2010) .
 - ¹² Benjamin E. Feldman, Jens Martin, Amir Yacoby, *Nature Physics* **5**, 889 (2009) .
 - ¹³ S. Ihnatsenka and G. Kirczenow, *Phys. Rev. B* **80**, 201407(R) (2009) .
 - ¹⁴ Hengyi Xu, T. Heinzl, and I. V. Zozoulenko, *Phys. Rev. B* **80**, 045308 (2009) .
 - ¹⁵ Wen Long, Qing-Fen Sun, and Jian Wang, *Phys. Rev. Lett.* **101**, 166806 (2008) .
 - ¹⁶ D. A. Abanin and L. S. Levitov, *Science* **317**, 641 (2007); J. R. Williams, L. Dicarlo, C. M. Marcus, *Science* **317**, 638 (2007) .
 - ¹⁷ Jian Li and Shun-Qing Shen, *Phys. Rev. B* **78**, 205308 (2008) .
 - ¹⁸ Lei Jing, Jairo Velasco Jr., Philip Kratz, Gang Liu, Wenzhong Bao, Marc Bockrath, Chun Ning Lau, *Nano Lett.* **10**, 4000 (2010) .
 - ¹⁹ Biswanath Chakraborty, Anindya Das and A K Sood, *Nanotechnology* **20**, 365203 (2009) .
 - ²⁰ Supriyo Datta, *Electronic transport in mesoscopic systems*, Cambridge Uni. Press (1999) .
 - ²¹ N.V. Baranova, P.E. Markina, A.I. Kozlova, E.V. Sinitsynb, *J. Alloys and Compounds* **200**, 43 (1993) .
 - ²² M. S. Dresselhaus and G. Dresselhaus, *Adv. Phys.* **51**, 1 (2002) .
 - ²³ M. P. Lopez Sancho, J. M. Lopez Sancho, and J Rubio, *J. Phys. F: Met. Phys.* **14**, 1205 (1984); *ibid.* **15**, 851 (1985) .
 - ²⁴ D. H. Lee and J. D. Joannopoulos, *Phys. Rev. B* **23**, 4988 (1981); *ibid.* **23**, 4997 (1981) .
 - ²⁵ Marco Buongiorno Nardelli, *Phys. Rev. B* **60**, 7828 (1999) .
 - ²⁶ C. Ojeda-Aristizabal, M. Monteverde, R. Weil, M. Ferrier, S. Guéron, H. Bouchiat, *Phys. Rev. Lett.* **104**, 186802 (2010) .
 - ²⁷ N. Xu and J. W. Ding, *J. Phys.: Condens. Matter* **20**, 485213 (2008) .

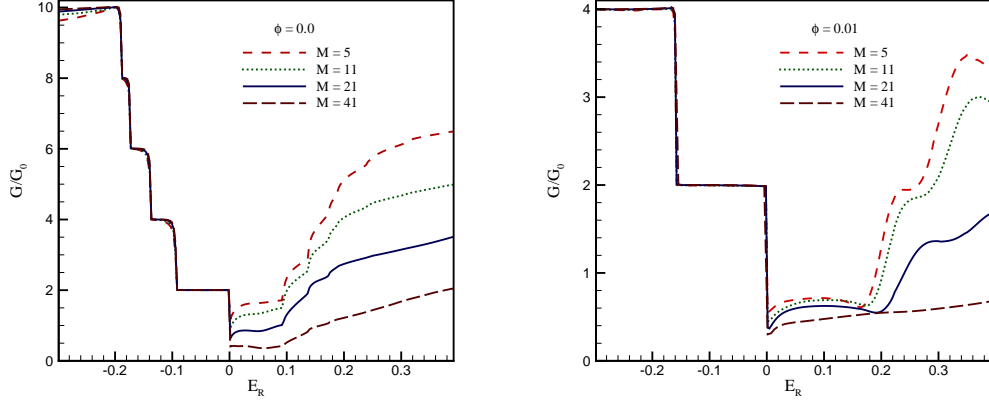


FIG. 2: (Color online) Conductance of a clean zBGNR as a function of E_R for various lengths with $E_L = -0.2$ for $\Delta = 0.0$ at $\phi = 0$ and $\phi = 0.01$.

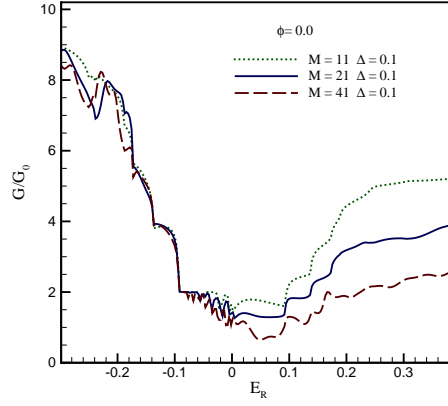


FIG. 3: (Color online) Conductance of a clean zBGNR with the asymmetry between two layers, as a function of E_R for various lengths with $E_L = -0.2$ at zero-magnetic field.

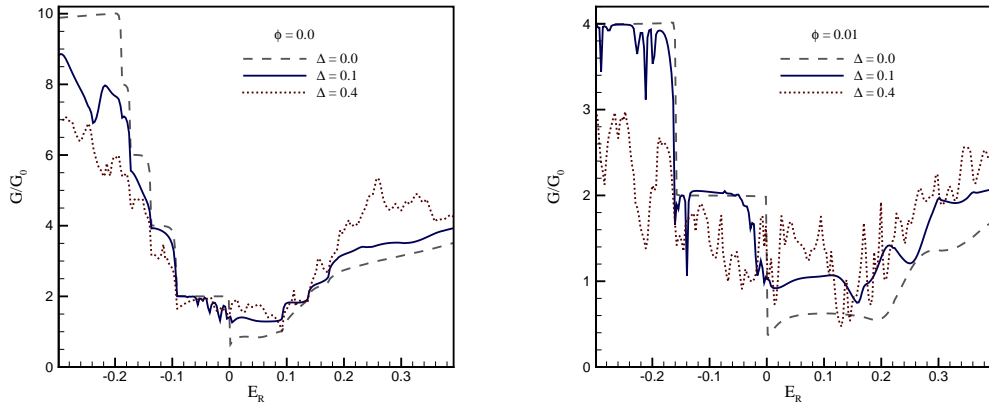


FIG. 4: (Color online) Conductance of a zBGNR as a function of E_R for $M = 21$, $E_L = -0.2$, and various Δ values at $\phi = 0$ and $\phi = 0.01$.

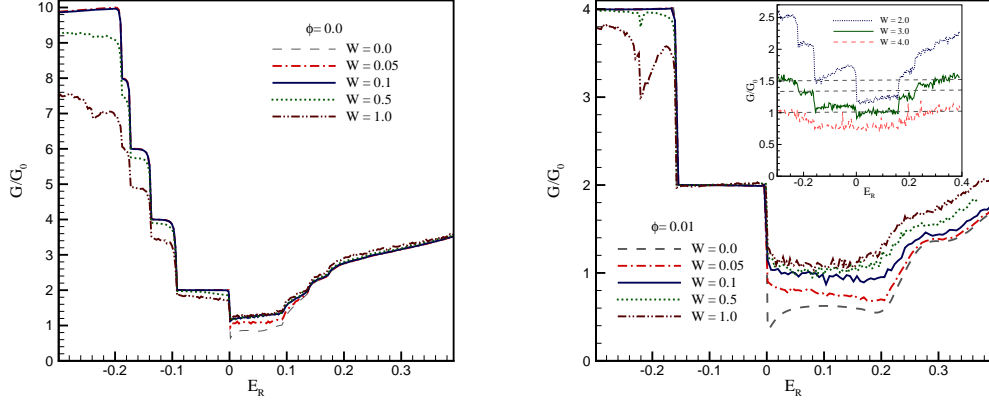


FIG. 5: (Color online) Conductance of a zBGNR as a function of E_R for $M = 21$, $E_L = -0.2$, and various on-site disorder strengths at $\phi = 0$ and $\phi = 0.01$.

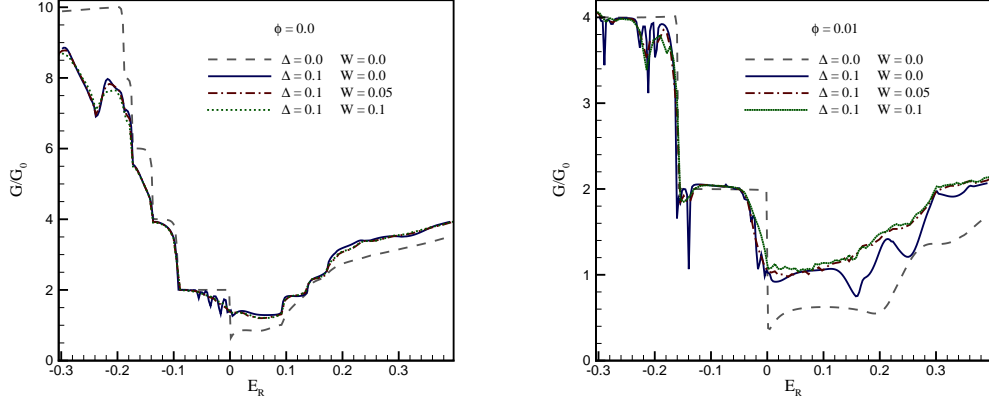


FIG. 6: (Color online) Conductance of a zBGNR as a function of E_R for $M = 21$, $E_L = -0.2$, $\Delta = 0.1$ and various on-site disorder strengths at $\phi = 0$ and $\phi = 0.01$.

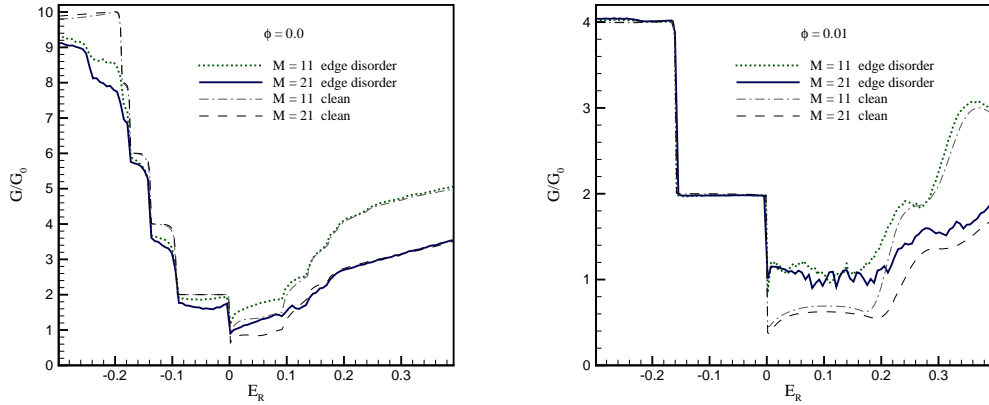


FIG. 7: (Color online) Edge disordered conductance of a zBGNR as a function of E_R in comparison with the clean system in the various values of the lengths for $E_L = -0.2$ at $\phi = 0$ and $\phi = 0.01$.